Enhanced kinetic inertness in the electrochemical interconversion of Cu(I) double helical to Cu(II) monomeric complexes†

Piersandro Pallavicini,*[a] Massimo Boiocchi,[b] Giacomo Dacarro[a] and Carlo Mangano[a]

Received (in Durham, UK) 12th January 2007, Accepted 21st March 2007
First published as an Advance Article on the web 3rd April 2007
DOI: 10.1039/b700488e

Three new ligands made of two iminoquinoline halves separated by an (*R*,*R*)-*trans*-1,2-cyclohexenediyl spacer have been synthesized. These ligands feature –OR functions appended in the 8-positions of the quinoline rings (R = *n*-alkyl). The ligands display a behaviour similar to that of their analogues that contain unsubstituted quinolines, forming a bistable system with copper. $[Cu_2\mathbf{L}_2]^{2+}$ helicates are obtained with Cu^+ and $[Cu\mathbf{L}]^{2+}$ monomers with Cu^{2+}, as shown by UV/Vis titrations, determination of complex formation constants, mass and NMR measurements, and X-ray crystallographic analysis. The OR groups are found to be non-coordinating, but the presence of such substituents on the quinoline rings slows the electrochemical interconversion of $[Cu_2\mathbf{L}_2]^{2+}$ into $[Cu\mathbf{L}]^{2+}$. In particular, oxidation of $[Cu_2\mathbf{L}_2]^{2+}$ gives a reversible two-step profile in cyclic voltammetry experiments, due to the formation of the Cu^{2+} helicate $[Cu_2\mathbf{L}_2]^{4+}$, that does not evolve into $[Cu\mathbf{L}]^{2+}$ in the CV experiment time scale.

Introduction

Using an external trigger to control movements at the molecular level is a goal that has been extensively studied in recent years.[1] In this perspective we have recently published a series of papers in which bis-bidentate ligands of the bis(iminoheterocycle) type have been used with the Cu(II)/Cu(I) couple to obtain bistable systems capable of fast electrochemically driven self-assembling/disassembling processes.[2–8] In particular, using *trans*-1,2-cyclohexyl or *cis*-1,2-cyclohexyl spacers between the two bidentate halves of the ligand, double helical Cu(I) complexes of the $[Cu_2\mathbf{L}_2]^{2+}$ type and monomeric Cu(II) complexes of the $[Cu\mathbf{L}]^{2+}$ type have been obtained.[2,5] In the former Cu^+ is four-coordinated, with a (distorted) tetrahedral geometry, and in the latter Cu^{2+} is six-coordinated with a tetragonal geometry, with the ligand arranged in a (distorted) square planar disposition around the metal centre and two solvent molecules completing the coordination sphere. These complexes can be interconverted electrochemically with a process that is sketched in Scheme 1, evidencing that the whole cycle is the sum of two classical EC (electrochemical–chemical) processes. In the $[Cu_2\mathbf{L}_2]^{2+}$ and in the $[Cu\mathbf{L}]^{2+}$ complexes the coordination number and geometry of copper is dramatically different and, accordingly, a different *E* value is found for the Cu(II)/Cu(I) redox couples: *e.g.* E_{ox} = 615 mV *vs.* Fc^+/Fc and E_{red} = −20 mV *vs.* Fc^+/Fc in the case of **t-BIQ**, *i.e.* the ligand with *trans*-1,2-cyclohexyl as a spacer and quinoline as the heterocycle. In addition, the chemical self-assembling and disassembling processes (see Scheme 1) are fast. As a consequence, in a cyclic voltammetry (CV) experiment, separate and irreversible oxidation and reduction events are obtained. The return waves are not observed because both the transient $[Cu\mathbf{L}]^+$ and $[Cu_2\mathbf{L}_2]^{4+}$ undergo self-assembling and disassembling processes that are complete in less than 20 ms.[5] This behaviour corresponds to electrochemical hysteresis, and these systems have been proposed as models for molecular memories. Moreover, we have found that changing the heterocycle or the spacer between the bidentate halves leaves unchanged the fast nature of the self-assembling/disassembling processes

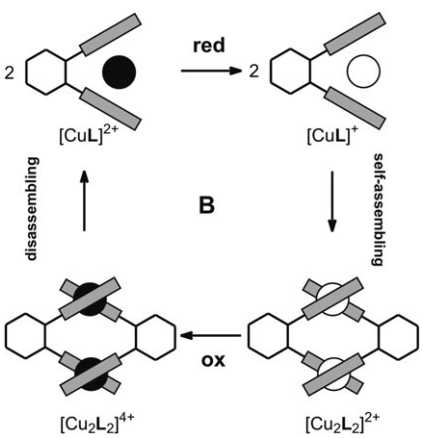

Scheme 1 Pictorial representation of the electrochemically controlled self-assembling and disassembling cycle of bis(imineheterocycle) copper helicates. Reduction and oxidation (electrochemical processes) are followed by rearrangements (chemical processes).

[a] *Dipartimento di Chimica Generale, Università di Pavia, viale Taramelli, 12, 27100 Pavia, Italy. E-mail: piersandro.pallavicini@unipv.it; Fax: +39 0382 528544; Tel: +39 0382 987329*
[b] *Centro Grandi Strumenti, Università di Pavia, via Bassi, 21, 27100 Pavia, Italy*

† Electronic supplementary information (ESI) available: Species distribution for the $[\mathbf{L}_2Cu_2]^{2+}$ helicates as a function of Cu^+ concentration, NMR spectra of the $[\mathbf{L}_2Cu_2](ClO_4)_2$ helicates in CD_3CN, series of absorption spectra and *Q vs. t* profile for a controlled potential coulometry experiment (oxidation of $[\mathbf{L1}_2Cu_2]^{2+}$). See DOI: 10.1039/b700488e

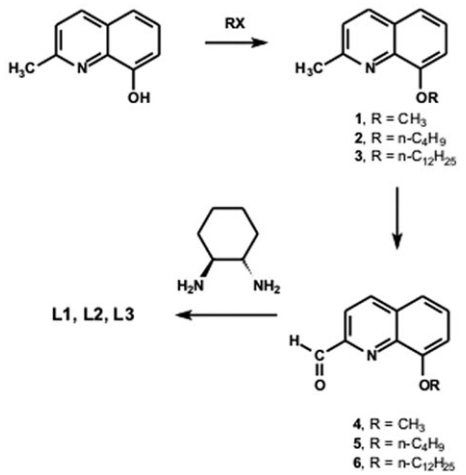

Scheme 2 Synthetic steps for the preparation of **L1**–**L3**. Details are described in the Experimental section.

but leads to significant changes in the E_{ox} and E_{red} values and in their difference ΔE, that represents the amplitude of the bistability interval of the system in a hysteresis cycle: *e.g.* E_{ox} = 530 and 723 mV, and E_{red} = 20 and −241 mV *vs.* Fc^+/Fc, respectively, for the *trans*- and *cis*-bis(iminophenanthridine) ligands **t-BIP** and **c-BIP**.[5] In addition, it should be mentioned that other authors have described comparable bistable systems, based on the Cu(II)/Cu(I) couple and on bis-bidentate ligands of the polypyridine type, capable of forming monomeric Cu(II) complexes and dimeric double helical Cu(I) species.[9–13] These papers show that subtle differences in the ligand structure (even in the peripheral part, not involved in coordination) may originate either fast or slow rearranging processes to follow the electrochemical steps. With this background, we have prepared three new ligands, **L1**–**L3**, containing the same binding set as **t-BIQ**, but with additional –OR groups in the 8-position of the quinoline heterocycles. The synthetic approach to these ligands is easy (see Scheme 2), it starts from commercially available products and it is of general application, *i.e.* it allows the introduction in this type of molecules of a variety of R groups, opening the path to the attainment of function-bearing Cu(I) helicates and Cu(II) monomers. Through electrochemical, spectrophotometric and X-ray diffraction experiments we have demonstrated that the ligand–copper systems are bistable, forming Cu(II) monomers and Cu(I) double helical dimers. However, even the introduction of the smallest R group, $-CH_3$, leads to the enhancement of the kinetic inertness of the transient $[Cu_2\mathbf{L}_2]^{4+}$ species, resulting in a slow rearrangement process following the electrochemical oxidation of $[Cu_2\mathbf{L}_2]^{2+}$.

Experimental

X-Ray crystal diffraction

Ambient-temperature intensity data (graphite-monochromatized Mo-Kα X-radiation; λ = 0.71073 Å) were collected on a Bruker-Axs SMART-APEX CCD based diffractometer (crystal of the **L1** complex) and on a conventional Enraf Nonius CAD4 four-circle diffractometer (crystal of the **L2** complex).

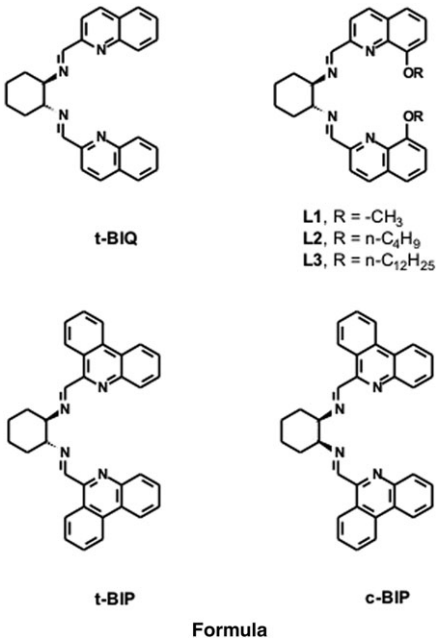

Frames collected by the CCD based system were processed with the SAINT software (Bruker-Axs Inc.) and intensities were corrected for Lorentz and polarization effects; absorption effects were empirically evaluated by the SADABS software[14] and absorption correction was applied to the data (0.69 and 0.89, min. and max. transmission factors). Data reductions (including intensity integration, background, Lorentz and polarization corrections) for intensities collected by the CAD4 system were performed using the WinGX package.[15] Absorption effects were evaluated with the psi-scan method[16] and absorption corrections were applied to the data (0.71 and 0.75, min. and max. transmission factors). Crystal structures were solved by direct methods (SIR 97)[17] and refined by full-matrix least-squares procedures on F^2 using all reflections (SHELXL 97).[18] All non-hydrogen atoms were refined with anisotropic temperature factors; hydrogens were placed at calculated positions using the appropriate AFIX instructions and refined using a riding model. Crystal data and details on the crystallographic study are reported in Table 1. The X-ray diffraction quality of the **L2** crystal complex imposed the use of soft restraints during the least-squares procedures, in order to avoid the convergence of the refinement towards structural models showing chemically unacceptable crystallographic features. In particular geometrical restraints have been applied to the atom sites forming the two quinoline moieties and restraints on the anisotropic displacement parameters have been applied both at the atoms of the quinoline rings and at the perchlorate oxygens.

CCDC reference numbers 641164 and 641165.

For crystallographic data in CIF or other electronic format see DOI: 10.1039/b700488e

Synthesis

2-Methylquinolin-8-ol, iodomethane, 1-bromobutane, 1-bromododecane and (*R*,*R*)-cyclohexane-1,2-diamine were purchased from Fluka or Aldrich and used as such.

Table 1 Crystal data for molecular complexes

	$[Cu^{I}_2\mathbf{L1}_2](ClO_4)_2$	$[Cu^{I}_2\mathbf{L2}_2](ClO_4)_2$
Formula	$C_{56}H_{56}Cl_2Cu_2N_8O_{12}$	$C_{68}H_{80}Cl_2Cu_2N_8O_{12}$
M	1231.09	1399.40
Colour	Dark blue	Dark violet
Crystal system	Trigonal	Orthorhombic
Space group	$P3_121$ (no. 152)	$I222$ (no. 23)
a/Å	14.1796(13)	13.8593(16)
b/Å	14.1796(13)	12.1710(19)
c/Å	25.0073(24)	20.9144(20)
V/Å^3	4354.3(7)	3527.8(8)
Z	3	2
μ(Mo-Kα)/mm^{-1}	0.892	0.742
D_c/cm^{-3}	1.408	1.317
2θ Range/°	3–50	2–60
Measured reflections	25 689	6568
Unique reflections	4869	5147
R_{int}	0.055	0.022
Strong data $I_0 > 2\sigma(I_0)$	2406	2479
Refined parameters	361	209
$R1$, $wR2$ (strong data)	0.089, 0.243	0.064, 0.137
$R1$, $wR2$ (all data)	0.156, 0.285	0.148, 0.178
GOF	0.974	0.992
Max., min. residuals/e Å^{-3}	0.47, −0.41	0.41, −0.34
Flack x parameter	0.02(5)	−0.03(3)

8-Methoxy-2-methylquinoline (1). A solution of 2-methylquinolin-8-ol (10.0 g, 63 mmol) in 20 mL of anhydrous ethanol was added dropwise to a stirred solution of NaOEt (prepared *in situ* from 1.6 g of sodium in 30 mL of anhydrous ethanol), under nitrogen. After 1 h, 3.9 mL of iodomethane (8.92 g, 63 mmol) were added dropwise and the reaction mixture was heated to reflux overnight, then filtered. Ethanol was removed on a rotary evaporator. The residue was dissolved in dichloromethane (100 mL) and washed with 2 × 100 mL water. The organic layer was dried over Na_2SO_4 and filtered. Removal of the solvent under reduced pressure yielded 8.5 g of a white solid (78%). Mass (ESI): m/z 174 $[M + H]^+$. ^{1}H NMR ($CDCl_3$): δ 8.05 (d, 1H), 7.83 (d, 1H), 7.58 (t, 1H), 7.48 (d, 1H), 7.38 (d, 1H) (H of the quinoline rings), 4.08 (s, 3H, –OCH_3), 2.80 (s, 3H, –CH_3).

8-Butoxy-2-methylquinoline (2). Compound **2** was prepared as **1** from 8.0 g (50 mmol) 2-methylquinolin-8-ol and 8.6 mL (10.97 g, 80 mmol) 1-bromobutane, yielding 6.2 g of white crystals (73%). Mass (ESI): m/z 216 $[M + H]^+$. ^{1}H NMR ($CDCl_3$): δ 8.02 (d, 1H), 7.81 (d, 1H), 7.54 (t, 1H), 7.47 (d, 1H), 7.36 (d, 1H) (H of the quinoline rings), 4.12 (d, 2H, OCH_2), 2.79 (S, 3H, –CH_3), 2.10 (m, 2H, OCH_2CH_2), 1.55 (m, 2H, $OCH_2CH_2CH_2$), 0.89 (t, 3H, –CH_2CH_3).

8-Dodecyloxy-2-methylquinoline (3). Compound **3** was prepared as **1**, except for a longer reaction time (2 days), by reacting 5.00 g (31.5 mmol) 2-methylquinolin-8-ol and 7.83 g (31.5 mmol). Crude product was also purified by column chromatography on alumina with hexane–ethyl acetate as eluent (3 : 2), yielding 5.4 g of **3** (52.5%) as a white waxy solid. Mass (ESI): m/z 328 $[M + H]^+$. ^{1}H NMR ($CDCl_3$): δ 8.02 (d, 1H), 7.81 (d, 1H), 7.54 (t, 1H), 7.47 (d, 1H), 7.36 (d, 1H) (H of the quinoline rings), 4.15 (t, 2H, OCH_2), 2.79 (s, 3H, –CH_3), 2.09 (m, 2H, OCH_2CH_2), 1.56 (m, 2H, $O(CH_2CH_2CH_2)$, 1.5–1.2 (m, 18H, CH_2 of the dodecyl chain), 0.87 (t, 3H, CH_3 of the dodecyl chain).

8-Methoxyquinoline-2-carbaldehyde (4). Compound **4** was prepared according to a described procedure[19] from **1** (3.0 g, 17.3 mmol), and purified by column chromatography on silica gel with ethyl acetate–hexane (3 : 2 v/v) as eluent to give 2.61 g of product as yellow crystals (80%). Mass (ESI): m/z 188 $[M + H]^+$, 220 $[M + MeOH + H]^+$ (hemiacetal). ^{1}H NMR ($CDCl_3$): δ 10.22 (s, 1H, CHO), 8.25 (d, 1H), 8.11 (d, 1H), 7.57 (t, 1H), 7.48 (d, 1H), 7.15 (d, 1H) (H of the quinoline rings), 4.35 (s, 3H, OCH_3). Elemental analysis. Calc. for $C_{11}H_9NO_2$: C, 70.58; H, 4.85; N, 7.48. Found: C, 70.60; H, 4.85; N, 7.47%.

8-Butoxyquinoline-2-carbaldehyde (5). Compound **5** was prepared as for **4**, from 2.8 g (13 mmol) **2**, and purified by column chromatography on silica gel with ethyl acetate–hexane (1 : 1) as eluent to give 2.46 g (83%) of product as yellow crystals. Mass (ESI): m/z 230 $[M + H]^+$, 262 $[M + MeOH + H]^+$ (hemiacetal). ^{1}H NMR ($CDCl_3$): δ 10.25 (s, 1H, CHO), 8.26 (d, 1H), 8.10 (d, 1H), 7.58 (t, 1H), 7.48 (d, 1H), 7.18 (d, 1H) (H of the quinoline rings), 4.32 (t, 2H, OCH_2–), 2.10 (m, 2H, OCH_2CH_2), 1.56 (m, 2H, $OCH_2CH_2CH_2$), 0.90 (t, 3H, –CH_3). Elemental analysis. Calc. for $C_{14}H_{15}NO_2$: C, 73.34; H, 6.59; N, 6.11. Found: C, 73.34; H, 6.61; N, 6.12%.

8-Dodecyloxyquinoline-2-carbaldehyde (6). Compound **6** was prepared as above for **4** from 2.5 g (7.6 mmol) of **3**, and purified by column chromatography on silica gel with hexane–ethyl acetate (4 : 1) as eluent, yielding 1.4 g of product (53.7%) as a yellow solid. Mass (ESI): m/z 342 $[M + H]^+$, 374 $[M + MeOH + H]^+$ (hemiacetal). ^{1}H NMR ($CDCl_3$): δ 10.29 (s, 1H, CHO), 8.27 (d, 1H), 8.06 (d, 1H), 7.60 (t, 1H), 7.46 (d, 1H), 7.15 (d, 1H) (H of the quinoline rings), 4.30 (t, 2H, OCH_2), 2.07 (m, 2H, OCH_2CH_2), 1.57 (m, 2H, $O(CH_2)_2CH_2$), 1.45–1.19 (m, 18H, CH_2 of the dodecyl chain), 0.88 (t, 3H, CH_3 of the dodecyl chain). Elemental analysis. Calc. for $C_{22}H_{31}NO_2$: C, 77.38; H, 9.15; N, 4.10. Found: C, 77.40; H, 9.16; N, 4.08%.

(1*R*,2*R*)-*N*,*N*′-Bis[1-(8-methoxyquinolin-2-yl)meth-(*E*)-ylidene]cyclohexane-1,2-diamine (L1). Ligand **L1** was prepared following a described procedure[2,3] from **2** (1.2 g, 6.4 mmol) and (1*R*,2*R*)-cyclohexane-1,2-diamine (0.36 g, 3.18 mmol), yielding 1.44 g of **L1** (89%) as a yellow solid. Mass (ESI): m/z 453 $[M + H]^+$. ^{1}H NMR ($CDCl_3$): δ 8.64 (s, 2H, HC═N), 8.09 (d, 2H, J = 8.8 Hz), 8.02 (d, 2H, J = 8.8 Hz), 7.41 (dd, 2H, J = 8.3, 7.8 Hz), 7.31 (d, 2H, J = 8.3 Hz), 7.01 (d, 2H, J = 7.8 Hz) (H of the quinoline rings), 4.07 (s, 6H, OCH_3), 3.64 (m, 2H, CH(N)–CH(N) of the cyclohexane ring), 1.5–1.9 (m, 8H, CH_2 of the cyclohexane ring). Elemental analysis. Calc. for $C_{28}H_{28}N_4O_2$: C, 74.32; H, 6.24; N, 12.37. Found: C, 74.29; H, 6.23; N, 12.25%.

(1*R*,2*R*)-*N*,*N*′-Bis[1-(8-butoxyquinolin-2-yl)meth-(*E*)-ylidene]-cyclohexane-1,2-diamine (L2). Ligand **L2** was prepared as above for **L1** from 1.41 g (6.2 mmol) **5** and 352 mg (3.1 mmol) (1*R*,2*R*)-cyclohexane-1,2-diamine, to give 1.46 g (88%) of product as a yellow solid. Mass (ESI): m/z 537 $[M + H]^+$. ^{1}H NMR ($CDCl_3$): δ 8.61 (s, 2H, HC═N), 8.08 (d, 2H, J = 8.8 Hz), 8.01 (d, 2H, J = 8.8 Hz), 7.39 (t, 2H, J = 7.8 Hz),

7.30 (d, 2H, J = 7.8 Hz), 7.02 (d, 2H, J = 7.8 Hz) (H of the quinoline rings), 4.22 (s, 4H, OCH_2), 3.66 (m, 2H, CH(N)–CH(N) of the cyclohexane ring), 2.0–1.5 (m, 16H, CH_2 of the cyclohexane ring and CH_2 of the butyl chains), 1.03 (t, 6H, CH_3 of the butyl chain). Elemental analysis. Calc. for $C_{34}H_{40}N_4O_2$: C, 76.09; H, 7.51; N, 19.43. Found: C, 76.06; H, 7.49; N, 19.41%.

(1*R*,2*R*)-*N*,*N*′-Bis[1-(8-dodecyloxyquinolin-2-yl)meth-(*E*)-ylidene]cyclohexane-1,2-diamine (L3). **L3** was prepared with a different synthetic procedure with respect to **L1** and **L2**. A solution of 43.5 mg (0.38 mmol) (1*R*,2*R*)-cyclohexane-1,2-diamine was added dropwise to a solution of 290 mg (0.85 mmol) **6** in 5 mL of CH_3OH, stirring vigorously. The reaction mixture was kept under stirring overnight, and a yellow oil separated from the solution. The oil was isolated by decantation, washed with 5 mL diethyl ether and dried under vacuum, yielding 219.4 mg (76%) of **L3**. Mass (ESI): m/z 761 $[M + H]^+$. ^{1}H NMR ($CDCl_3$): δ 8.61 (s, 2H, HC=N), 8.07 (d, 2H, J = 8.8 Hz), 8.01 (d, 2H, J = 8.8 Hz), 7.39 (dd, 2H, J = 8.3, 7.8 Hz), 7.30 (d, 2H, J = 8.3 Hz), 7.01 (d, 2H, J = 7.8 Hz) (H of the quinoline rings), 4.21 (s, 4H, OCH_2), 3.66 (m, 2H, CH(N)–CH(N) of the cyclohexane ring), 2.0–1.3 (m, 48H, CH_2 of the cyclohexane ring and CH_2 of the C_{12} chains), 0.89 (t, 6H, CH_3 of the C_{12} chain). Elemental analysis. Calc. for $C_{50}H_{72}N_4O_2$: C, 78.90; H, 9.53; N, 7.31. Found: C, 78.91; H, 9.55; N, 7.35%.

Metal complexes. $[\mathbf{L1}_2Cu_2](ClO_4)_2$ and $[\mathbf{L2}_2Cu_2](ClO_4)_2$ were prepared by dissolving a ~50 mg sample of the chosen ligand in 3 mL dry acetonitrile, and by adding the stoichiometric amount of $[Cu(CH_3CN)_4]ClO_4$. A dark blue-violet solution was obtained, that was allowed to evaporate in air, to give blue–violet crystals of the products. These were collected by suction filtration, dried under vacuum and found suitable for X-ray diffraction experiments. A similar procedure for **L3** yielded a waxy solid, that was not isolated. Analogous synthetic procedures were applied to try to isolate solid Cu(II) complexes of the three ligands, but, in all cases, the obtained green solutions yielded only oily films.

Electrochemistry and spectroelectrochemistry

Electrochemical measurements (cyclic voltammetry, CV, and controlled potential coulometry, CPC) were performed with a BAS 100B/W instrument. In CV studies (CH_3CN solution, 0.1 mol L^{-1} $(t\text{Bu})_4NClO_4$), a three-electrode cell was used, with a platinum electrode as the working electrode, a silver/silver ion electrode as the reference (clean silver wire into an electrode filling solution of CH_3CN made 10^{-2} M in $AgNO_3$, and 0.1 M in $(t\text{Bu})_4NClO_4$), and a platinum wire as the auxiliary electrode. Scan rates were in the 50–2000 mV s^{-1} range. The examined complexes were prepared *in situ* by adding in 1 : 1 molar ratio the chosen ligand and either $[Cu(CH_3CN)_4]ClO_4$ or $Cu(CF_3SO_3)_2$ (both ~10^{-3} M). CPC experiments were performed on solutions of $[Cu^{I}_2(\mathbf{L})_2](ClO_4)_2$ and $[Cu^{II}(\mathbf{L})](CF_3SO_3)_2$ prepared *in situ*. 40 mL of solutions ~2 × 10^{-4} mol L^{-1} were used for each experiment. A platinum gauze was used as the working electrode, the auxiliary electrode compartment was separated from the working compartment by a glass chamber, filled with CH_3CN (0.1 mol L^{-1}) in $(t\text{Bu})_4NClO_4$. The reference electrode (a silver/silver ion electrode as for CV experiments), was calibrated through CV experiments prior to CPC. The spectra of the solutions in the working cell were taken during the electrolysis by a quartz fiber optic probe (Hellma, 661.602-UV) connected to the diode-array spectrophotometer, with an optical path of 10 mm.

Titrations

Titrations were performed on 25 mL samples of CH_3CN solution made 2 × 10^{-4} M in the chosen ligand by microadditions of either $[Cu(CH_3CN)_4]ClO_4$ or $Cu(CF_3SO_3)_2$ solutions in CH_3CN. The concentration of the metal solution to be added was chosen so that 1 : 1 molar ratio with respect to ligand was obtained after the addition of 150 μL. Additions were made by 10 μL portions. After each addition, a ~2.5 mL portion of the titrated solution was transferred into a quartz cuvette, a spectrum was recorded and the portion was quickly transferred back to the bulk. Experiments were carried out on ligand and metal solutions deaerated with a N_2 flux prior to titrations. The solutions were also kept under a nitrogen atmosphere.

Instrumentation

Mass spectra (ESI) were recorded on a Thermo Finnigan LCQ Advantage Max, NMR spectra on a Bruker AMX 400 spectrometer. UV/Vis spectra were recorded on a Hewlett-Packard 8452A diode array spectrophotometer.

Results and discussion

1 Cu(I) helicate complexes

The tendency of **L1**–**L3** to form double helical complexes with Cu(I) has been verified by means of spectrophotometric titrations, made on ligand solutions in CH_3CN by addition of substoichiometric quantities of $[Cu(CH_3CN)_4]ClO_4$ (see Experimental section for titrations details). Upon addition of Cu^+, the titrated solutions take a blue–violet colour, due to a large MLCT absorption in the visible, with λ_{max} at 586, 578 and 572 nm for **L2**, **L3** and **L4**, respectively (see also Table 1). The band intensity increases up to 1 : 1 stoichiometry, and when excess Cu^+ is added no further variation is observed, obtaining a series of superimposable spectra. This behaviour is exemplified in Fig. 1, that reports the obtained series of spectra in the case of **L1** and that, in the inset, reports also the absorbance at 586 nm *vs.* molar ratio profile, displaying a steep increase and a plateau at molar ratio >1. Of course a 1 : 1 molar ratio corresponds to an authentic 2 : 2 stoichiometry, as demonstrated by X-ray diffraction and by MS-ESI experiments, that display for the three ligands peaks corresponding to $[Cu_2\mathbf{L}_2]^{2+}$ and to $\{[Cu_2\mathbf{L}_2]ClO_4\}^+$. From the spectrophotometric titrations it has been possible to calculate the formation constants of the $[Cu_2\mathbf{L}_2]^{2+}$ species by means of the Hyperquad data treatment package.[20] Data refinement has evidenced that, although with a small weight in the species distribution, also the $[Cu\mathbf{L}_2]^+$ species forms, at least at low metal : ligand molar ratios, in agreement also with the non-perfect linearity of the

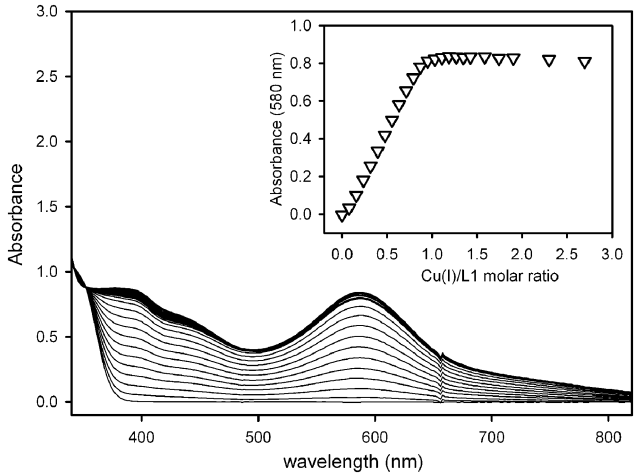

Fig. 1 Spectrophotometric titration of **L1** with substoichiometric quantities of Cu^+ (acetonitrile solution, ClO_4^- salt). On addition of Cu^+ the spectra increase in absorbance until reaching a plateau at 1 : 1 (corresponding to 2 : 2) ligand : metal molar ratio. The insert reports the absorbance values at 580 nm *vs.* the metal : ligand molar ratio.

ascending part of the absorbance *vs.* ratio profile (see inset of Fig. 1). Formation constants are collected in Table 2. Distribution diagrams may be drawn, reporting the percentage of ligand contained in each species with respect to total ligand, as a function of Cu^+ : **L** molar ratio (see ESI,† Fig. S1 and S2). As an example, in the case of **L1**, with a ligand concentration identical to that used to obtain the series of spectra reported in Fig. 1 (2.21×10^{-4} M), at a 1 : 1 Cu^+ : **L1** molar ratio the helical complex $[\mathbf{L1}_2Cu_2]^{2+}$ is at 96% and $[\mathbf{L1}_2Cu]^+$ at 4%, while addition of a slight excess of Cu^+ obviously displays the distribution towards 100% of $[\mathbf{L1}Cu_2]^{2+}$.[21] Similar features are found for the distribution diagrams in the case of **L2** and **L3**. Accordingly, solutions containing **L1**–**L3** and Cu^+ in 1 : 1 molar ratio can be considered as solutions containing the helicate complex, while the presence of the $[L_2Cu]^+$ species may be neglected in the interpretation *e.g.* of the spectrophotometric and electrochemical results. The λ_{max} values for the MLCT bands reported in Table 1 are to be compared with what observed for the helicates $[(\mathbf{t\text{-}BIQ})_2Cu_2]^{2+}$ (536 nm, ε = 3600 M^{-1} cm^{-1}), $[(\mathbf{t\text{-}BIP})_2Cu_2]^{2+}$ (558 nm, ε = 6250 M^{-1} cm^{-1}) and $[(\mathbf{c\text{-}BIP})_2Cu_2]^{2+}$ (570 nm, ε = 6400 M^{-1} cm^{-1}).[3] In the case of the **L1**–**L3** helicates, the λ_{max} value is shifted to longer wavelengths. However, subtle changes in the disposition of the N_4 donor set may strongly influence the λ_{max} value of the MLCT band, as indicated by the differences between the *cis*- and *trans*-isomers of ligand **BIP**. Of course also the electron-donating effect exerted by the –OR fragment probably plays a role in shifting to longer wavelengths with respect to **t-BIQ** the position of the MLCT absorption maximum in the helicates of **L1**–**L3**. In particular, the donor ability of the two iminoquinoline chelating units is expected to be increased and the energy of the LUMO of the iminoquinoline systems to be lowered. The bulkiness of the substituent on the oxygen atom plays an opposite role, shifting the MLCT absorption maximum to shorter wavelengths for **L2** and **L3** complexes, probably due to a sterical effect not allowing a metal–ligand interaction as efficient as for **L1**. This is reflected also in the $\log K$ values, and in particular on the step relative to the equilibrium $[L_2Cu]^+ + Cu^+ = [L_2Cu_2]^{2+}$, *i.e.* the step in which the second Cu^+ cation is added to the system making it to self-assemble in a closed, double helical form, from an open, monometallic species. The $\log K$ sequence 6.4, 6.2 and 5.6 is found for **L1**, **L2**, **L3**. The soft nature of the Cu^+ cation and its tendency to form tetrahedral complexes suggest that any coordinating role of the oxygen atom should be ruled out. This observation is fully confirmed by the determination of the crystal and molecular structure of $[\mathbf{L1}_2Cu_2](ClO_4)_2$ and $[\mathbf{L2}_2Cu_2](ClO_4)_2$, in which the O–Cu distances are clearly non-bonding (2.809/2.757 Å and 2.863 Å for the **L1** and **L2** complexes). Examination of the crystal and molecular structures (Fig. 3 and 4, and pertinent discussion) also evidences that the disposition of the ligands is symmetrical, *i.e.* the two iminoquinoline halves of each ligand are equivalent, and also the two ligands are equivalent. This observation is not obvious, as it should be remembered that **t-BIQ** is able to form, in the solid state, both a symmetrical and a dissymmetrical helicate, the latter featuring two non-equivalent iminoquinoline halves for each ligand.[2] The structures determined by X-ray diffraction are consistent with what is found in the NMR spectra of the complexes, that display a main set of signals, with those belonging to the quinoline and imine protons shifted with respect to the free ligands. In particular, the HC=N imino proton is shifted upfield to 8.3, 7.8 and 7.7 ppm for the helicates formed by **L1**, **L2** and **L3**, respectively ($\Delta\delta$ = −0.34, −0.89, −0.99). The examination of the crystal and molecular structures of the helicates formed by **L1** and **L2** suggests that this shift is due to the particular position of the –HC=N– moieties of one ligand, that are parallel and at short distance with respect to the quinolines belonging to the other intertwined ligand. The distances between the two mean planes are 3.11(1) and 3.33(1) Å for $[\mathbf{L1}_2Cu_2]^{2+}$ and 3.11(1) Å for $[\mathbf{L2}_2Cu_2]^{2+}$). It must also be stressed that beside the main set of signals, the NMR spectra of the helicates display a second set of signals of lower intensity, in which two twin subsets are found. Most of the signals fall under the main set and this split subset cannot be fully described (see also ESI,† Fig. S3 and S4). However, for the aromatic protons some signals are found at ppm values at which they do not superimpose to other signals, and, in particular, the imino protons give origin to two

Table 2 Absorption spectral data and formation constants for **L1**–**L3** complexes

	L1	L2	L3
λ_{max} $[L_2Cu_2]^{2+}$ (ε)[a]	586 (3820)	578 (4284)	572 (5840)
λ_{max} $[LCu]^{2+}$ (ε)[b]	760 (150)	752 (140)	754(170)
$\log K_{21}$[c]	11.0(0.1)	11.85(0.05)	10.5(0.1)
$\log K_{22}$[d]	17.4(0.1)	18.08(0.05)	16.1(0.1)

[a] Spectral data for Cu(I) helicates: λ_{max} in nm, ε in M^{-1} cm^{-1}. [b] Spectral data for Cu(II) complexes: λ_{max} in nm, ε in M^{-1} cm^{-1}. [c] $\log K_{21}$: logarithmic constants relative to the formation of $[L_2Cu]^+$, *i.e.* to equilibrium $2\,L + Cu^+ = [L_2Cu]^+$, with uncertainties in parenthesis. [d] Logarithmic constants relative to the formation of $[L_2Cu_2]^{2+}$, *i.e.* to equilibrium $2\,L + 2\,Cu^+ = [L_2Cu_2]^{2+}$, with uncertainties in parenthesis.

isolated low field twin singlets (9.45 + 9.70, 9.42 + 9.60 and 9.38 + 9.73 for **L1**, **L2** and **L3** helicates, respectively), whose integration allows to evaluate the quantity of ligand being employed in this minor form with respect to total ligand. We measured ~5, ~8 and ~10% for the complexes of **L1**, **L2** and **L3**, respectively. The non-equivalence of the quinoline signals and the measured percentages suggest that this subset is originated by the $[\mathbf{L}_2\mathrm{Cu}]^+$ form, that, according to the calculated formation constants, is present at the equilibrium, at the 5×10^{-4}–10^{-3} M concentrations used for NMR spectra, in compatible percent values.[21] It should be noticed that in the case of ligand **t-BIQ** a similar NMR spectrum was found (one main set plus a minor set split into two subsets), but only when the enantiomeric *RR* + *SS* mixture of the ligands was used, and that the minor form has been attributed to the $[(\mathbf{L1}\text{-}RR)(\mathbf{L1}\text{-}SS)\mathrm{Cu}_2]^{2+}$ complex, [3] a species that in the present work is obviously ruled out, as only enantiopure (*R*,*R*)-*trans*-1,2-cyclohexanediamine was used for the synthesis of the ligands. Finally, it is worth mentioning that solutions of Cu^+ helicates are indefinitely stable, as we checked spectrophotometrically, if maintained at room temperature, in CH_3CN exposed to air, light and humidity. Moreover, a 10^{-3} M solution of $[\mathbf{L2}_2\mathrm{Cu}_2]^{2+}$ in acetonitrile has been treated with water (1 : 9 v/v H_2O–CH_3CN) and no variation in the UV/Vis spectrum was recorded in a 12 h period, demonstrating the stability of these complexes towards hydrolysis of the imino groups or oxidation to Cu(II) species.

2 Cu(II) complexes

Spectrophotometric titrations have been used to study also the coordination properties of **L1**–**L3** towards Cu^{2+}. Addition of substoichiometric quantities of $Cu(CF_3SO_3)_2$ to acetonitrile solutions of the any of the three ligands results in the formation of green-yellowish solutions, whose spectra reveal both an intense CT transition in the 400–500 nm range (ε = 1100–1400 M^{-1} cm^{-1}) and a low-intensity d–d band at 780–750 nm (ε = 140–170 M^{-1} cm^{-1}). Fig. 2 reports the series of spectra obtained in the case of **L1**. The inset of Fig. 2 reports the absorbance at 400 nm *vs.* the **L1** : Cu^{2+} molar ratio, showing that a plateau is reached at 1 : 1 stoichiometry. MS-ESI measurements confirm that what is obtained is the $[\mathbf{L}\mathrm{Cu}]^{2+}$ complex for all three ligands, showing molecular peaks corresponding to $[\mathbf{L}\mathrm{Cu}]^{2+}$ and to $\{[\mathbf{L}\mathrm{Cu}]CF_3SO_3\}^+$. Calculation of the formation constants of these species from the spectrophotometric data was not possible, due to some unavoidable and spontaneous reduction of Cu^{2+} to Cu^+ at low metal : ligand molar ratio. This reduction originates traces of the Cu^+ helicate, whose intense and large absorptions slightly affect the Abs *vs.* Cu^+ : L molar ratio profiles thus not allowing satisfactory refinement of the absorption data. The maxima of absorption of the d–d band (Table 1) are at longer wavelengths, if compared with the complex $[\mathbf{t\text{-}BIQ}\mathrm{Cu}]^{2+}$ (668 nm, ε = 105 M^{-1} cm^{-1}), $[\mathbf{t\text{-}BIP}\mathrm{Cu}]^{2+}$ (700 nm, ε = 105 M^{-1} cm^{-1}) and $[\mathbf{c\text{-}BIP}\mathrm{Cu}]^{2+}$ (716 nm, ε = 240 M^{-1} cm^{-1}).[4] In these complexes we have reported that the ligands surround Cu^{2+} in distorted square planar disposition, and the overall geometry is tetragonal, with two apical CH_3CN molecules completing the coordination sphere. According to the crystal structure found for $[\mathbf{t\text{-}BIQ}\mathrm{Cu}](CF_3SO_3)_2$, the disposition of the N_4 donor set is distorted from square planar towards tetrahedral to avoid repulsion between the phenyl rings of the two quinolines of the ligand.[1] In particular, the carbons in the 8 positions would be very close, if the disposition of the donors around Cu^{2+} was perfectly planar. Accordingly, with ligands **L1**–**L3**, that bear –OR substituents in the 8 positions, we expect an increased distortion of the N_4 donor set from planarity and a less efficient Cu–N interaction in their complexes, resulting in the unusually long wavelengths found for absorption maxima.

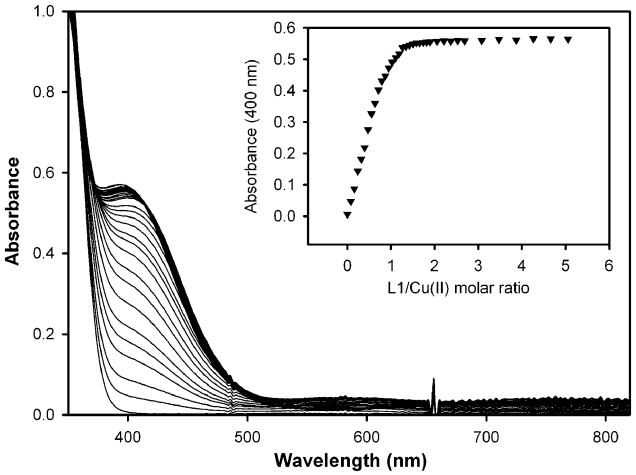

Fig. 2 Series of spectra in the spectrophotometric titration of **L1** with Cu^{2+} (acetonitrile solution, $CF_3SO_3^-$ salt). On addition of substoichiometric quantities of Cu^{2+} cation, the band at ~410 nm increases in intensity, reaching a plateau at 1 : 1 ligand : metal molar ratio (see inset for a plot of Abs_{400} *vs.* ligand : metal molar ratio).

3 Crystal and molecular structure of the Cu(I) helicates $[\mathbf{L1}_2\mathrm{Cu}_2]^{2+}$ and $[\mathbf{L2}_2\mathrm{Cu}_2]^{2+}$

X-Ray diffraction studies allowed to determine the molecular structure of the Cu(I) complexes of **L1** and **L2** (as perchlorate salts) that are shown in Fig. 3 and 4. Both **L1** and **L2** ligands form dimeric 2 : 2 metal–ligand double helical molecular cations. Each copper cation is coordinated by four nitrogens of two iminoquinoline chelating units belonging to two different ligands. Copper displays a distorted tetrahedral coordination. The mean $Cu\text{–}N_{imino}$ distances, 2.103(15) Å in $[\mathbf{L1}_2\mathrm{Cu}_2]^{2+}$ and 2.028(4) in $[\mathbf{L2}_2\mathrm{Cu}_2]^{2+}$ complexes are slightly longer than the mean $Cu\text{–}N_{quinoline}$ ones, that are 2.037(9) Å in $[\mathbf{L1}_2\mathrm{Cu}_2]^{2+}$ and 2.019(4) in $[\mathbf{L2}_2\mathrm{Cu}_2]^{2+}$. However, these values are in the range already observed for tetrahedrally coordinated Cu(I) centers in iminoquinoline complexes.[2,3,5]

The oxygen atoms of the O–Me and O–But groups moieties are significantly distant from the metal centers. In the $[\mathbf{L1}_2\mathrm{Cu}_2]^{2+}$ molecular cation the two non-symmetrically equivalent Cu–O distances are 2.754(10) and 2.808(12) Å. In the $[\mathbf{L2}_2\mathrm{Cu}_2]^{2+}$ cation the O atoms symmetrically related and placed at 2.863(6) Å from the metal center. Therefore, in both complexes the O atoms can be considered definitely non-coordinating.

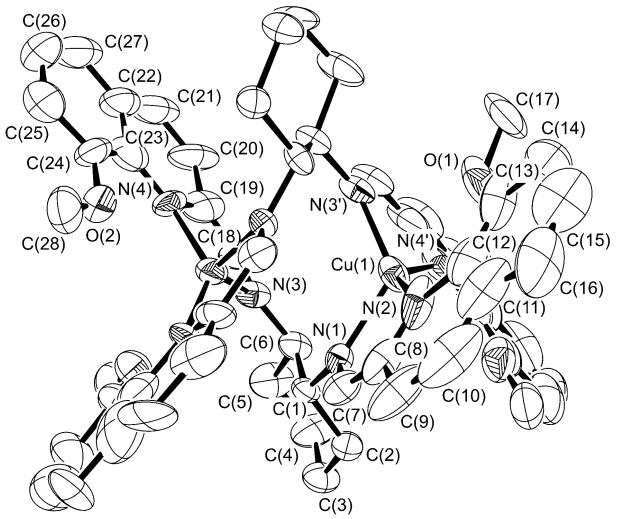

Fig. 3 An ORTEP view of the $[\mathbf{L1}_2Cu_2](ClO_4)_2$ salt (thermal ellipsoids are drawn at the 20% probability level; H atoms and perchlorate counterions are omitted for clarity). Atom labels are reported only for the asymmetric unit (half of the molecule) and for all nitrogens around Cu(1). Selected geometrical features (Å, °) around the metal centre: Cu(1)–N(1) 2.066(9), Cu(1)–N(2) 2.069(16), Cu(1)–N(3′) 2.009(9), Cu(1)–N(4′) 2.137(13); N(1)–Cu(1)–N(2) 81.3(6), N(1)–Cu(1)–N(3′) 122.9(3), N(1)–Cu(1)–N(4′) 110.7(4), N(2)–Cu(1)–N(3′) 127.7(4), N(2)–Cu(1)–N(4′) 139.9(6), N(3′)–Cu(1)–N(4′) 79.0(6); symmetry code: (′) = y, x, $1 - z$.

In both $[\mathbf{L1}_2Cu_2]^{2+}$ and $[\mathbf{L2}_2Cu_2]^{2+}$ the 1,2-diaminocyclohexane is in its *R*,*R* form and this results in a *M* handedness of the double helical molecular dimers. The Cu–Cu separation is 3.71(1) and 3.76(1) Å in $[\mathbf{L1}_2Cu_2]^{2+}$ and $[\mathbf{L2}_2Cu_2]^{2+}$, respectively. The $[\mathbf{L1}_2Cu_2]^{2+}$ molecular cation exhibits C_2 point symmetry because the two **L1** ligands and the two metal centers are related by a crystallographic twofold rotation axis that passes through the molecular centroid. Moreover, the $[\mathbf{L2}_2Cu_2]^{2+}$ molecular cation results arranged according to a higher molecular symmetry, because the centroid of the molecule lies at the origin of the crystallographic unit cell. The three crystallographic twofold rotation axes that pass through the cell origin give the complex D_2 point symmetry and define as asymmetric unit only one Cu(I) and half of the **L2** ligand.

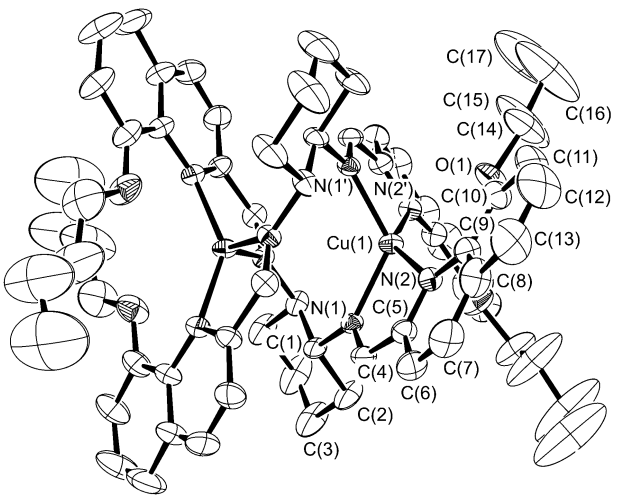

Fig. 4 An ORTEP view of the $[\mathbf{L2}_2Cu_2](ClO_4)_2$ complex (thermal ellipsoids are drawn at the 20% probability level; H atoms and perchlorate counterions are omitted for clarity). Atom labels are reported only for the asymmetric unit (a quarter of the molecule) and for all nitrogens around Cu(1). Selected geometrical features (Å, °) around the metal centre: Cu(1)–N(1) 2.019(4), Cu(1)–N(2) 2.028(4); N(1)–Cu(1)–N(2) 82.5(2), N(1)–Cu(1)–N(1′) 125.3(2), N(1)–Cu(1)–N(2′) 115.4(2), N(2)–Cu(1)–N(2′) 142.3(2); symmetry code: (′) = x, $1 - y$, $1 - z$.

4 Electrochemistry

The electrochemical behaviour of Cu^+ helicates and Cu^{2+} monomers has been examined by means of cyclic voltammetry experiments, carried out on acetonitrile solutions prepared *in situ* by addition of $[Cu(CH_3CN)_4]ClO_4$ (for Cu(I) helicates) or of $Cu(CF_3SO_3)_2$ (for Cu(II) monomers) in 1 : 1 molar ratio with respect to the chosen ligand. It has to be remembered that in the cases of bis(iminoheterocycle) ligands such as **t-BIQ** or **t-BIP** and **c-BIP**, identical CV profiles where obtained from their Cu(I) and Cu(II) complexes, with separate and irreversible oxidation and reduction profiles, due to the fast disassembling of the transient $[L_2Cu_2]^{4+}$ (from oxidation of Cu(I) helicates) into $[LCu]^{2+}$ and to the fast self-assembling of the transient $[LCu]^+$ (from the reduction of the Cu(II) monomer) into $[L_2Cu_2]^{2+}$.[2,5] In the case of the **L1**–**L3** complexes a different CV profile is instead obtained for the Cu(I) helicates with respect to the Cu(II) monomers. The electrochemical behaviour is almost identical on going from **L1** to **L3** complexes, and the case of **L1** is examined in detail as an example. Cyclic voltammetry experiments on $[\mathbf{L1}_2Cu_2]^{2+}$ in acetonitrile (0.1 M TBAP as the background electrolyte) disclose a reversible two-wave signal, shown in Fig. 5(A), with $E_{1/2}$ values of 133 mV (ΔE = 105 mV) and 382 mV (ΔE = 90 mV) *vs.* Fc^+/Fc. On changing the sweep rate between 50 and 2000 mV s^{-1}, the same profile is obtained, due to the reversible single electron oxidation of each Cu(I) centre, first to the Cu(I)–Cu(II) species $[\mathbf{L1}_2Cu_2]^{3+}$ and then to the bis-Cu(II) species $[\mathbf{L1}_2Cu_2]^{4+}$. Reversibility of the CV profile, even at the slowest sweep rate, indicates that the two species do not undergo any chemical rearrangement on the time scale of the CV experiments (from ~100 to ~1 s), *i.e.* the disassembling of $[\mathbf{L1}_2Cu_2]^{4+}$ is slow and the double helical architecture is maintained during the CV runs. It has to be remembered that, on the contrary, in the case of the complexes of the plain iminoquinoline ligands **BIQ** and **BIP**, the oxidation of the Cu(I) helicates was found irreversible (*i.e.* with no return wave) even at the fastest scan rate (10–20 × 10^3 mV s^{-1}) due to the fast disassembling process following the helicate oxidation. Examination of the CV behaviour of the Cu(II) complex $[\mathbf{L1}Cu]^{2+}$ discloses another type of profile (Fig. 5(B)). An irreversible reduction peak is observed at E = −154 mV *vs.* Fc^+/Fc, that does not feature a return wave, as in the case of the Cu(II) monomeric complexes of **BIQ** and **BIP**. However, on returning to positive potential values, the two reversible waves pertaining to the Cu(I) helicate $[\mathbf{L1}_2Cu_2]^{2+}$ are found again: in this case, the self-assembling process following the reduction of $[\mathbf{L1}Cu]^{2+}$ to $[\mathbf{L1}Cu]^+$ is fast on the time scale of the electrochemical

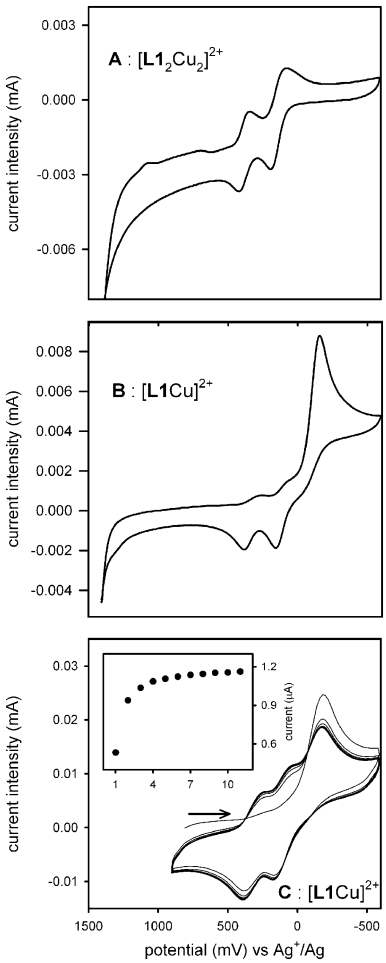

Fig. 5 (A) Cyclic voltammetry run on the Cu(I) helicate $[\mathbf{L1}_2Cu_2]^{2+}$, starting from $E = 0$ *vs.* Fc^+/Fc and scanning first towards positive potentials. Scan rate = 200 mV s^{-1}. (B) Cyclic voltammetry run on the Cu(II) monomer $[\mathbf{L1}Cu]^{2+}$, starting from $E = 0$ *vs.* Fc^+/Fc and scanning first towards negative potentials. Scan rate = 200 mV s^{-1}. (C) Series of 10 CV cycles on the Cu(II) monomer $[\mathbf{L1}Cu]^{2+}$, starting from 800 mV *vs.* Fc^+/Fc and scanning first towards negative potentials, with 200 mV s^{-1} scan rate; the arrow indicates graphically the starting point of the experiment and the scan direction; the current intensity of the wave at −154 mV decreases, while the current intensity of the reversible waves increases; the inset shows the current measured on the reduction peak of the reversible signal at $E_{1/2} = 133$ mV (due to the *in situ* formed $[\mathbf{L1}_2Cu_2]^{2+}$ helicate) as a function of the number of cycles; the huge increase observed on going from cycle 1 to cycle 2 is due to the fact that obviously no $[\mathbf{L1}_2Cu_2]^{2+}$ species was present on starting the experiment.

experiment. The difference in the speed of the two rearrangement processes following the electrochemical ones is supported also by the results found on running repeated CV cycles on the Cu(II) monomer: starting the CV experiment from $E = 800$ mV no signal is observed before reaching the potential of reduction of $[\mathbf{L1}Cu]^{2+}$ (−154 V), while on returning to positive potential values the signal relative to $[\mathbf{L1}_2Cu_2]^{2+}$ appears and this species is accumulated at the electrode on cycling, as indicated by the increase with time of the current intensity of its signals and by the decrease of the intensity of the $[\mathbf{L1}Cu]^{2+}$ signal (see in the inset the reduction current intensity at $E = 80$ mV *vs.* number of cycles). The increased slowness of the rearrangement process following oxidation (disassembling) with respect to that following reduction (self-assembling) is not unexpected: in a series of molecular machines based on the Cu(II)/Cu(I) couple, the molecular movements following oxidation were found much slower than those following reduction.[22] The latter take place on d^{10} species, while the former on d^9 species, and it can be proposed that crystal field activation energy is responsible for the increased slowness of rearrangements involving Cu^{2+} species.[23] However, it has to be stressed that the difference in inertness after oxidation between the helicates of **L1**–**L3** and those of **BIQ** and **BIP** ligands is striking. The increased inertness of the **L1**–**L3** transient Cu(II) helicates can probably be ascribed to the closed and intertwined nature of the complexes, in which the additional –OR groups sterically hinder the disassembling step. However the disassembling process following oxidation develops and is complete on longer times. We carried out controlled potential coulometry (CPC) experiments on $[\mathbf{L1}_2Cu_2]^{2+}$, oxidising the bulk electrochemical solution at 500 mV *vs.* Fc^+/Fc and we also recorded a series of UV/Vis spectra on the solution to check the evolution of the complex species. The electrolysis process was complete in ~1 h, as we observed the passage of 98% of the expected current (two moles of electron per mole of $[\mathbf{L1}_2Cu_2]^{2+}$) in 3800 s (ESI,† Fig. S5, inset). The recorded UV/Vis spectra series (ESI,† Fig. S5) show the disappearance of the MLCT band of the Cu(I) helicate and the formation of the bands relative to the Cu(II) monomer. Moreover, at the end of the CPC process (3800 s), the recorded spectra were found to be superimposable to that of an authentic solution of $[\mathbf{L1}Cu]^{2+}$. Finally, the potential values found for the oxidation and reduction of the **L1**–**L3** complexes are to be noted. The obtained values are summarized in Table 3, referred to the Fc^+/Fc couple.[24] On stepping from **L1** to **L3**, what is observed is the tendency to shift to lower values of the potential relative to irreversible reduction of $[\mathbf{L}Cu]^{2+}$, and an opposite trend for the reversible oxidation of $[\mathbf{L}_2Cu_2]^{2+}$. These small potential shifts are probably connected with the slightly different arrangement of the N_4 donor sets around the metal centres, as can be expected on stepping from R = $–CH_3$ to R = $–C_{12}H_{25}$. However, a striking difference is seen with respect to the E_{red} and E_{ox} potentials found for the Cu^{2+} complex of **t-BIQ**, *i.e.* −20 mV and 615 mV *vs.* Fc^+/Fc, respectively,[5] evidencing the

Table 3 Electrochemical data from CV measurements for the Cu^+ and Cu^{2+} complexes of **L1**–**L3**

	$[L_2Cu_2]^{2+}$	$[LCu]^{2+}$
L1[a]	382 (90) 133 (105)	−154
L2[a]	419 (80) 202 (78)	−186
L3[a]	427 (170) 182 (148)	−234

[a] Potential values (mV) are referred to the Fc^+/Fc couple. $E_{1/2}$ values are given for $[L_2Cu_2]^{2+}$ species; E_{red} (single irreversible peak) values are given for $[LCu]^{2+}$ species. The peak separations for the reversible signals are reported in parentheses. Instrumental uncertainty is ±5 mV.

overall electron enriching effect exerted by –OR on the ligand framework of the systems described in the present work.

Acknowledgements

This work was financially supported by Università di Pavia (FAR 2005) and by MIUR (project FIRB RBNE019H9K-002 and COFIN2005 National Program).

References

1 (*a*) B. Champin, P. Mobian and J.-P. Sauvage, *Chem. Soc. Rev.*, 2007, **36**, 358; (*b*) J. Berna, G. Bottari, D. A. Keigh and E. M. Perez, *Pure Appl. Chem.*, 2007, **79**, 39; (*c*) S. Saha and J. F. Stoddart, *Chem. Soc. Rev.*, 2007, **36**, 77; (*d*) V. Balzani, A. Credi, S. Silvi and M. Venturi, *Chem. Soc. Rev.*, 2006, **35**, 1135; (*e*) C. Anda, C. Bazzicalupi, A. Bencini, A. Bianchi, P. Fornasari, C. Giorgi, B. Valtancoli, C. Lodeiro, A. J. Parola and F. Pina, *Dalton Trans.*, 2003, 1299.
2 V. Amendola, L. Fabbrizzi, L. Linati, C. Mangano, P. Pallavicini, V. Pedrazzini and M. Zema, *Chem.–Eur. J.*, 1999, **5**, 3679.
3 V. Amendola, L. Fabbrizzi, C. Mangano, P. Pallavicini, E. Roboli and M. Zema, *Inorg. Chem.*, 2000, **39**, 5803.
4 V. Amendola, L. Fabbrizzi and P. Pallavicini, *Coord. Chem. Rev.*, 2001, **216–217**, 435.
5 V. Amendola, L. Fabbrizzi, L. Gianelli, C. Maggi, C. Mangano, P. Pallavicini and M. Zema, *Inorg. Chem.*, 2001, **40**, 3579.
6 V. Amendola, L. Fabbrizzi, P. Pallavicini, E. Sartirana and A. Taglietti, *Inorg. Chem.*, 2003, **42**, 1632.
7 V. Amendola, L. Fabbrizzi, E. Mundum and P. Pallavicini, *Dalton Trans.*, 2003, 773.
8 V. Amendola, M. Boiocchi M, Y. Diaz Fernandez, C. Mangano and P. Pallavicini, *Collect. Czech. Chem. Commun.*, 2003, **68**, 1647.
9 J.-P. Gisselbrecht, M. Gross, J. M. Lehn, J.-P. Sauvage, R. Ziessel, C. Piccinni-Leopardi, J. M. Arrieta, G. Germain and M. Van Meerssche, *Nouv. J. Chim.*, 1984, **8**, 661.
10 Y. Yao, M. W. Perkovic, D. P. Rillema and C. Woods, *Inorg. Chem.*, 1992, **31**, 3956.
11 K. T. Potts, M. Keshavarz-K, F. S. Tham, H. D. Abruña and C. R. Arana, *Inorg. Chem.*, 1993, **32**, 4422.
12 K. T. Potts, M. Keshavarz-K, F. S. Tham, H. D. Abruña and C. R. Arana, *Inorg. Chem.*, 1993, **32**, 4450.
13 R. Ziessel, A. Harriman, J. Suffert, M. T. Youinou, A. De Cian and J. Fischer, *Angew. Chem., Int. Ed. Engl.*, 1997, **36**, 2509.
14 G. M. Sheldrick, *SADABS*, Program for area detector adsorption correction, Institute for Inorganic Chemistry, University of Göttingen, Germany, 1996.
15 L. J. Farrugia, *J. Appl. Crystallogr.*, 1999, **32**, 837.
16 A. C. T. North, D. C. Phillips and F. S. Mathews, *Acta Crystallogr., Sect. A: Cryst. Phys., Diffr., Theor. Gen. Crystallogr.*, 1968, **24**, 351.
17 A. Altomare, M. C. Burla, M. Camalli, G. L. Cascarano, C. Giacovazzo, A. Guagliardi, A. G. G. Moliterni, G. Polidori and R. Spagna, *J. Appl.Crystallogr.*, 1999, **32**, 115.
18 G. M. Sheldrick, *SHELX97 Programs for Crystal Structure Analysis*, University of Göttingen, Germany, 1997.
19 G. P. Xue, P. B. Savage, K. E. Krakowiak, R. M. Izatt and J. S. Brasdshaw, *J. Heterocycl. Chem.*, 2001, **38**, 1453.
20 P. Gans, A. Sabatini and A. Vacca, *Talanta*, 1996, **43**, 1739.
21 In the case of a 5×10^{-4} M solution of both ligand and Cu^+ the following percentage of $[\mathbf{L}_2Cu_2]^{2+}$ may be calculated: **L1**: 96.3, **L2**: 94.2, **L3**: 90.8%. In the case of a 10^{-3} M solution, the calculated percentages of $[\mathbf{L}_2Cu_2]^{2+}$ are **L1**: 97.5, **L2**: 96.6, **L3**: 93.5%.
22 (*a*) A. Livoreil, C. O. Dietrich-Buchecker and J.-P. Sauvage, *J. Am. Chem. Soc.*, 1994, **116**, 9399; (*b*) D. J. Cardenas, A. Livoreil and J.-P. Sauvage, *J. Am. Chem. Soc.*, 1996, **118**, 11980; (*c*) I. Poleschak, J.-M. Kern and J.-P. Sauvage, *Chem. Commun.*, 2004, 474.
23 F. Basolo and R. G. Pearson, *Mechanisms of Inorganic Reactions: A Study of Metal Complexes in Solution*, Wiley, New York, 2nd edn, 1967.
24 CV measurements have been run using an $AgNO_3$/Ag electrode as the reference. $E_{1/2}$ values have been successively referred to the Fc^+/Fc couple by measuring the ferrocene CV profile in the same electrochemical setup. We found $E_{1/2}(Fc^+/Fc)$ = 94 mV *vs.* $AgNO_3$/Ag in agreement with what has been reported in the literature for the Ag^+/Ag electrode and Fc^+/Fc in acetonitrile (see *Handbook of Analytical Chemistry*, ed. L. Meites, McGraw Hill, New York, 1963, and T. Gennett, D. F. Milner and M. J. Weaver, *J. Phys. Chem.*, 1985, **89**, 2787).